Effects of Transcranial Ultrasound Stimulation Pulsed at 40 Hz on Aβ Plaques and Brain Rhythms in 5XFAD Mice

Mincheol Park
Gwangju Institute of Science and Technology
Gia Minh Hoang
Gwangju Institute of Science and Technology
Thien Nguyen
Gwangju Institute of Science and Technology
Eunkyung Lee
Gwangju Institute of Science and Technology
Hyun Jin Jung
KBRI: Korea Brain Research Institute
Youngshik Choe
KBRI: Korea Brain Research Institute
Jae Gwan Kim
Gwangju Institute of Science and Technology
Tae Kim (tae-kim@gist.ac.kr)
Gwangju Institute of Science and Technology https://orcid.org/0000-0003-0201-5401

Research

Keywords: transcranial ultrasound stimulation, gamma band oscillation, amyloid- β plaques, Alzheimer's disease

Posted Date: July 26th, 2021

DOI: https://doi.org/10.21203/rs.3.rs-734856/v1

Abstract

Background

Alzheimer's disease (AD) is the most common cause of dementia characterized by amyloid-β (Aβ) plaques and tauopathy. Reducing Aβ has been considered a major AD treatment strategy in pharmacological and non-pharmacological treatments. The impairment in the gamma oscillations, which play an important role in perception and cognitive function, has been shown in mouse AD models and human patients. Recently the therapeutic effect of gamma entrainment treatment on the AD mouse model was reported. Given that ultrasound is an emerging modality of neuromodulation, we investigated the effect of ultrasound stimulation pulsed at gamma frequency (40Hz) on an AD mouse model.

Methods

We implanted electroencephalogram (EEG) electrodes and a piezo-ceramic disc ultrasound transducer on the skull surface of 6-months-old 5XFAD and wild-type control mice (n=12 and 6, respectively). Six 5XFAD mice were treated with daily two-hour ultrasound stimulation at 40Hz for two weeks, and the other six mice received sham treatment. Soluble and insoluble Aβ levels in the brain were measured by enzyme-linked immunosorbent assay. Spontaneous EEG gamma power was computed by wavelet analysis, and the brain connectivity was examined with phase-locking value and cross-frequency phase-amplitude coupling.

Results

We found that total Aβ 42 and 40 levels, especially insoluble, in the treatment group decreased compared to that of the sham treatment group. The reduction in the number of Aβ plaques in PIL also has been shown. In addition, spontaneous gamma power was increased, and brain connectivity was improved.

Conclusions

These results suggest that the transcranial ultrasound-based gamma-band entrainment technique can be an effective therapy for AD by reducing the Aβ load and improving brain connectivity

Introduction

Alzheimer's disease (AD) is one of the most common neurodegenerative diseases affecting over 50 million people in the world characterized by cognitive deficits, impaired activities of daily living, and behavioral disturbance [1]. Two major pathological hallmarks of AD are the presence of extra-cellular senile plaques made by the accumulation of Aβ and intracellular neurofibrillary tangles from the deposition of hyper-phosphorylated tau protein [2–4]. In normal conditions, Aβ plaques are degraded by microglia and astrocyte [5] and the soluble Aβ is removed through the perivascular pathway [6, 7]. The progressive shift of brain Aβ soluble pools to insoluble and the impairment of plaque clearance function plays important roles in the onset and progression of AD. Although medications until now have failed to

prevent aggregation of amyloid ‘plaques’ in AD patients [8, 9], the pharmacological and non-pharmacological treatments based on the 'amyloid hypothesis' are still major methods of AD treatment, especially aiming at the reduction of accumulated Aβ [10]. In this study, we investigated the ultrasound-based gamma-band entrainment technique to reduce brain pathology in an AD mouse model.

The activity of neurons with different frequencies of gamma-band (~ 30-100Hz) oscillation are raised across multiple brain regions, where they are assumed to play an important role in perception, cognitive functions, such as attention, learning, memory encoding and retrieval [11, 12]. Gamma oscillations are produced by synaptic activity between GABAergic inhibitory interneurons and excitatory pyramidal cells [13–15]. The degeneration of spontaneous gamma synchronization and reduction in spontaneous gamma power have been typically shown in multiple AD mouse models [16–19] and human patients [20–22].

Recently, a technique based on gamma-band entrainment was used as a therapeutic treatment for AD. Iaccarino et al. [23] have shown that optogenetic stimulation and visual stimulation at 40 Hz decreased Aβ peptides and increased microglia clustering around Aβ plaques in the hippocampus and the visual cortex of 5xFAD mouse model, respectively. Besides, Martorell et al. [24] also have reported that multi-sensory gamma stimulation can reduce Aβ plaques and improve cognitive function. However, there is a lack of studies regarding the therapeutic effects of gamma-band entrainment by ultrasound stimulation in Alzheimer's disease. Transcranially delivered ultrasound can safely activate central neural circuits and exert neuroprotective effects on dementia [25–27]. In 2020, Bobola et al. [28] delivered transcranial focused ultrasound stimulation (tUS) with 2.0 MHz carrier frequency, 40 Hz pulse repetition frequency into 5XFAD mice for 1 hour per day at one hemispheric brain. They observed a reduction of Aβ plaques and activation of microglia co-localized with Aβ in the area of the treated brain [28]. Therefore, we hypothesized that gamma-band entrainment using 40 Hz ultrasound stimulation (US) could reduce Aβ load and increase spontaneous gamma oscillations and brain connectivity.

Methods

Animals preparation

All animals were housed in a temperature and humidity-controlled room at 20°C ± 2°C, 55% ± 5% under a 12:12 light-dark cycle. We used 6-month-old male 5XFAD mice expressing human Aβ peptide precursor gene with Swedish, Florida, and London mutations and PS1 with mutations M146L and L286V. All animal procedures have been approved by the ethics committee (GIST-2020-031), which is fulfilled with Association for Assessment and Accreditation of Laboratory Animal Care International guidelines.

Surgical preparation, electrode, and transducer implantation

5XFAD mice were anesthetized with 4% isoflurane and maintained with 0.5–1.5% isofluorane in a stereotaxic frame. Ketofen (0.1 mg/kg) was injected subcutaneously before surgery as an analgesic. Electrodes for electroencephalogram (EEG) were implanted on the frontal (AP = 1.0 mm; ML = 1.0 mm)

and parietal (AP = -3.5 mm; ML = 1.0 mm) areas of the skull (Fig. 1a) and connected to a premanufactured head mount (8402, Pinnacle Technology). A piezo-ceramic disc transducer (SMD07T03R411, Steiner & Martins Inc.) with two connecting wires was placed on top of the headmount layer and combined by dental cement (Fig. 1b).

Transcranial Ultrasound Stimulation (tUS) experiment

We used 12 male 5XFAD mice: treatment group (n = 6; Tg/Stim+) mice, sham treatment group (n = 6; Tg/Stim-), and wild-type mice (n = 6; WT). The tUS was performed every day for two weeks. We used the piezo-ceramic disc transducer implanted it to a mice head above the EEG electrode layer. The ultrasonic beam applied tUS at 40Hz (similar with gamma frequency oscillation) with a carrier frequency of 300 kHz and pulse length of 3 ms, for 200 ms each second, for 10 s followed by 30 s of no ultrasound, for 2 hours was delivered (Fig. 1c). The width of the ultrasound beam at each depth of brain tissue ranged from 5.5 to 6.0 mm. We used LabView (National Instruments Corporation, Texas, USA) to control the function generator. The signal generated by the function generator was amplified before it was transferred to the piezo-ceramic disc transducer. tUS pulsed at 40 Hz successfully induced EEG responses centered at 40 Hz, confirmed by averaging the ~ 1200 time-frequency plots for each mouse during 2 hours of stimulation (Fig. 1d).

EEG Recordings and Data Analysis

Mice were tethered to the recording system and habituated to the recording environment 24 hours before the recording (Fig. 1b). EEG of freely moving mice was recorded with a sampling rate at 2 kHz and a low-pass filter at 100 Hz (8200-K1-SL, Pinnacle Technology) from 00:00 to 08:00. To analyze the EEG data, we performed offline processing in the customized code for Matlab and Python. Spontaneous gamma power was examined at 30–80 Hz. Briefly, the signal was filtered by a second-order Butterworth filter with a higher and lower cut-off adjusted to 2 Hz above and 100 Hz below to remove a DC noise. Spontaneous gamma power was calculated by computing the power spectral density (PSD) using Welch's method and integrating PSD at the given frequency band using the composite Simpson's rule. The phase locking value (PLV) was calculated by applying the Hilbert transform with a determined frequency band and measuring the differences in the instantaneous phase between the frontal and parietal EEG signals. All analyses were done using a toolbox in MATLAB (Brainstorm, Mathworks). Cross-frequency phase-amplitude coupling (PAC) was calculated by Gaussian Copula PAC method and denoising.

Mouse brain preparation and enzyme-linked immunosorbent assay (ELISA)

Mice were deeply anesthetized by isoflurane and then transcardially perfused with phosphate-buffered saline (PBS). Brains were removed and dissected into two hemispheres. The right hemisphere was dissected by the brainstem, thalamus, hippocampus, cerebellum, and cortex and stored at -80°C until use. The cortical and hippocampal regions were dissected and homogenized in 20 mM Tris-HCl (pH 7.6) with 5 mM EDTA and protease inhibitor cocktail (P3100, GenDEPOT). The homogenates were centrifuged at 430,000 g for 20 min at 4°C to separate the soluble and insoluble Aβ. The supernatants were kept at

-20°C, and the pellet was resuspended in 5 mM guanidine-hydrochloride and 50 mM Tris-HCl (pH 7.6). After centrifugation at 430,000 g for 20 min at 4°C, the supernatants were saved at -20°C. Total protein was quantified by BCA assay (23225, Thermo Fisher Scientific). ELISA for soluble and insoluble Aβ was conducted following the manufacturer's instruction (Aβ42: KHB3441, Aβ40: KHB3481, Thermo Fisher Scientific).

Histology

The left hemisphere was fixed by 4% paraformaldehyde (PFA) overnight and placed in 30% sucrose solution until it sinks. The fixed brain tissues were cut in a coronal section (40 μm) with a cryostat (Leica). The brain sections were rinsed three times with PBS containing 1% Triton X-100 (PBST) for 10 min each in shaking at 120 rpm. Tissues were blocked by 3% normal donkey serum (D9633, Sigma Aldrich) in 0.5% PBST for 2hr incubation at room temperature. Primary antibodies used for microglia was rabbit anti-Iba1 (1:1,000, 019-19741, Wako) and the secondary was donkey anti-rabbit IgG (1:500, A31572, Invitrogen). Aβ deposits were stained by 1 mM Thioflavin S (T1892, Sigma Aldrich). The tissues were mounted onto a silane-coated slide glass (5116-20F, Muto Pure Chemicals), and the images were acquired by a confocal microscope (LSM880NLO, Carl Zeiss).

Results

- **Aβ loads in the cortex and hippocampus region changed after two weeks of transcranial ultrasound stimulation at 40 Hz**

In the pre- and infra limbic cortex (PIL), there was a significant decrease of total Aβ42 level in Tg/Stim + comparing with those of WT and Tg/Stim- groups ($p < 0.01$; Fig. 2a). In sub-fraction analysis, Tg/Stim + showed significant reduction in insoluble Aβ42 levels than Tg/Stim- ($p < 0.05$; Fig. 2a), whereas the soluble Aβ42 of Tg/Stim + increased. We also observed the decrease of total and soluble Aβ40 levels in Tg/Stim + group in comparison with Tg/Stim- group, but there was no significant difference (Fig. 2b).

In hippocampus, Aβ levels changed in a similar pattern, but the difference were not significant. Tg/Stim + showed a slight decrement of insoluble Aβ42 and Aβ40 levels in hippocampus while the soluble Aβ42 and Aβ40 of Tg/Stim + showed no statistically significant increment in comparison with Tg/Stim- group ($p > 0.05$; Fig. 2c-d).

We also examined the number of Aβ plaques and microglia by immunohistochemistry (Fig. 3a). In the pre- and infra limbic cortex, the numbers of Aβ plaques per unit area were diminished in Tg/Stim + compared with those of Tg/Stim-, but there is no significant ($p > 0.05$; Fig. 3b). Tg/Stim + showed a significant reduction in the microglia marker Iba1 intensity per unit area in PIL cortex than Tg/Stim- ($p < 0.05$; Fig. 3c).

- **Relative spontaneous gamma power and phase-locking value in electroencephalography changed after 2 weeks of transcranial ultrasound stimulation at 40 Hz**

We measured the effects of 2 weeks of ultrasound stimulation on the spontaneous gamma power in the AD mouse model. Power spectral analysis (Welch's method) was performed with a range of gamma frequencies (30–80 Hz). The gamma power was then normalized to the total power for relative gamma power. We performed repeated measure analysis of variance (RM ANOVA) to compare relative spontaneous gamma power at different time points. The relative gamma power at baseline in WT showed a significant increase compared with Tg/Stim + and Tg/Stim- ($p < 0.05$; Fig. 4a). Tg/Stim- showed a statistically significant decrement comparing with WT in relative gamma power on day 7 and day 14 ($p < 0.05$ and $p < 0.01$, respectively), on the other hand, the difference between WT and Tg/Stim + was no significant ($p > 0.05$; Fig. 4a). We also observed a statistically significant increment of relative gamma power in Tg/Stim + in comparison with Tg/Stim- group ($p < 0.05$; Fig. 4a).

Phase-locking value (PLV) was calculated at spontaneous gamma frequency, and the difference of PLV at day 7 versus baseline and day 14 versus day 7 was evaluated for each group to investigate the change of synchronization of spontaneous gamma between frontal and parietal. There was an increment in PLV from baseline to day 7 in WT group, but both Tg/Stim + and Tg/Stim- showed downward trends (Fig. 4b). In addition, from day 7 to day 14, phase-locking values in Tg/Stim + and WT showed an increasing trend, whereas those of Tg/Stim- remained in the reducing trend (Fig. 4b).

Cross-frequency phase-amplitude coupling changed after 2 weeks of transcranial ultrasound stimulation at 40 Hz

In phase-amplitude coupling (PAC), a decreased coupling of delta-phase (2–5 Hz; frontal EEG) and gamma-amplitude (30–80 Hz; parietal EEG) in Tg/Stim + at baseline (middle column) compared to those of wild type (WT, left column) or the last day of stimulation (Tg/Stim + at day 14, right column) (Fig. 5a upper panels and 5b). Theta-phase (5–8 Hz; parietal EEG) and gamma-amplitude (80–160 Hz; frontal EEG) was increased in Tg/Stim + in day 14 compared to those of WT or Tg/Stim + groups at baseline (Fig. 5a lower panels and 5c).

Discussion

Here we showed 14-day ultrasonic stimulation at 40 Hz gamma frequency decreased Aβ load in pre- and infra limbic cortex and hippocampus in an animal model of AD. In addition to the molecular and histologic improvement, we also found neurophysiological evidence of functional improvement, such as increased spontaneous gamma oscillations, PLV, and PAC throughout the treatment course. To the best knowledge of ours, this is the first report that ultrasound-based transcranial neuromodulation at gamma frequency has a therapeutic potential for AD.

Neuromodulation effects of ultrasound stimulation

Recent studies have already shown that ultrasound stimulation exerted neuroprotective effects. In 2018, Eguchi et al [25] have demonstrated that ultrasound stimulation with a pulse repetition frequency (PRF)

of 1 kHz could reduce amyloid-β plaque, increase cerebral blood flow (CBF), and affected endothelial nitric oxide (eNOS) that considered as an important therapeutic target in AD [5]. Additionally, Huang et al. have reported that LIPUS was effective for improving the density of dendritic spines, altering electrophysiological properties, and significantly increased the expression level of GluN2A in the hippocampus [26]. All of these findings provide strong evidence for the beneficial effects of ultrasonic neuromodulation.

tUS stimulation can entrain gamma band oscillations

Fast-spiking parvalbumin (PV) cells are GABAergic interneurons that express in ~ 40% of inhibitory interneurons and receive N-methyl-D-aspartate (NMDA) excitatory input from pyramidal cells [17, 29]. The regulation of FS–PV interneurons through GABAergic inhibitory synaptic activity onto excitatory pyramid cells generates and fine-tunes gamma oscillations [13–15]. Gamma oscillations in neural networks play an important role in the performance of a variety of perception, cognitive tasks, including the allocation of attention and working memory. Previous studies have already shown that the gamma oscillation reduced in Alzheimer's disease [17, 21]. In 2012, Verrett et al. have reported that the recovery of the gamma activity by increasing Nav1.1 expression in PV cells followed by the reduction of network hyper-synchronization and cognitive function loss in the AD animal model [17]. In our study, we observed that transcranial ultrasound stimulation at 40 Hz could entrain the gamma band oscillations. Relative gamma power increased significantly after 2 weeks of ultrasound stimulation, whereas non-treatment groups (Tg/Stim-) showed the significant decrement.

Aβ load decreased by tUS

The total Aβ levels (Aβ42 and Aβ40) in cortical areas and hippocampus reduced in Tg+/Stim + than Tg+/Stim- after two weeks of transcranial ultrasound stimulation. The decrement of insoluble Aβ42 in Tg/Stim + showed statistical significance in the cortex but not in the hippocampus, whereas soluble Aβ42 slightly but significantly increased. In terms of the amyloid beta level, therapeutic effects and potentially harmful changes appeared simultaneously. The relative toxicity of soluble and insoluble amyloid beta is controversial. Insoluble Aβ fibrils were aggregated from Aβ monomers and oligomers [30], and they can accumulate to form the amyloid plaques, which are known as pathological hallmarks in Alzheimer's disease. The aggregation of insoluble fibrils causes neuro-inflammation, which leads to the damages of neurites and decreases the Aβ clearance [31, 32]. The fibrillar plaques also causally related to the progressive neuritic abnormalities in amyloid precursor protein (APP) transgenic mice model [33, 34]. Indeed, our histological analysis showed the number of Aβ plaques in PIL reduced in Tg/Stim+, and the signal intensity of microglia decreased. We thought that the decreased insoluble Aβ could result in the reduced neuro-inflammation, or vice versa, in spite of increased soluble Aβ. However, amyloid oligomers are soluble and can spread widely throughout the brain. The soluble oligomers cause hyper-phosphorylation of the tau protein, which forms the neurofibrillary tangles (NFTs) and leads to neuronal synaptic dysfunction in Alzheimer's disease [35]. Aβ oligomers also induced the disruption of the neuritic cytoskeleton and accelerated the cytotoxic effects [36]. Both fibrils and soluble Aβ have found to induce cell death via different pathways. Oligomers induce cell death via apoptosis, whereas amyloid fibrils lead

to necrosis-like death [37]. Given that insoluble and soluble Aβ are pathogenic in different mechanisms, such as neuro-inflammation, synaptotoxicity, tau pathology, we may be able to suggest that the net effect of the tUS gamma entrainment might be therapeutic because we found a marker of neuro-inflammation was reduced and functional markers of neurophysiology was improved.

Functional improvement could be achieved by tUS

Recent studies have reported that the loss of EEG synchronization increased in AD patients and correlated with cognitive dysfunction [20–22]. The gamma-band entrainment technique could improve cognitive function and memory performance [23, 24]. Because transcranial ultrasound stimulation at 40 Hz could increase spontaneous gamma power, we investigated whether tUS have a functional improvement in a mouse model. PLV can reflect the functional impairment of connectivity effectively because only the phase excluding amplitude and frequency is considered. Our results showed a trend of decrement of PLV in the sham treatment group (Tg/Stim-) during two weeks; on the other hand, the direction of PLV changes in the treatment group (Tg/Stim+) changed from decrement (day 7-baseline) to increment (day 14-day 7), although there was no statistical significance. Two weeks of ultrasound stimulation might have contributed to the recovery of PLV. We also analyzed the cross-frequency phase-amplitude coupling (PAC) to see how the phase of low-frequency oscillations modulate high-frequency power, especially the gamma band. The local processing could be fine-tuned or influenced by the modulation of gamma activity within particular areas by low-frequency oscillation. Recent studies revealed that theta-phase high-gamma coupling correlates with working memory performance by manipulating the ordering of information during the working memory process [38, 39]. The impairment of theta-gamma coupling followed by memory deficits was reported by Goodman et .al in 2018 [40]. In our study, we observed the reduction of theta-gamma PAC of Tg/Stim + mice comparing with WT group at baseline. After 2 weeks of tUS stimulation, the theta-gamma coupling in Tg/Stim + in day 14 increased significantly in comparison with Tg/Stim + at baseline. Delta-gamma coupling also considered as a biomarker for the evaluation of generalized EEG suppression as well as network activity [41]. Our results showed an exaggeration of delta-gamma coupling in Tg/Stim + day 14 in comparison with Tg/Stim + at baseline. Taken together, all of these results support that gamma-band entrainment by tUS stimulation at 40 Hz can normalize PLV and cross-frequency coupling, implying improved brain connectivity and information processing.

Conclusion

In summary, we conclude that tUS brain stimulation at 40 Hz can be a potential therapeutic modality by reducing Aβ load and improving brain connectivity. However, understanding the exact mechanism of these results is beyond the scope of the current study. Further investigation about the neurobiology of these therapeutic effects is warranted.

Abbreviations

AD: Alzheimer's disease; Aβ: amyloid-β; EEG: electroencephalogram; WT: wild type; Tg/Stim+: 5xFAD with stimulation; Tg/Stim-: 5XFAD sham stimulation; tUS: transcranial ultrasound stimulation; PSD: power spectral density; PLV: phase locking value; PAC: phase-amplitude coupling; ELISA: enzyme-linked immunosorbent assay ; PBS: phosphate-buffered saline; PFA: paraformaldehyde; PIL: pre- and infra limbic; HPC: hippocampus; RM ANOVA: repeated measure analysis of variance; PRF: a pulse repetition frequency; CBF: cerebral blood flow; eNOS: endothelial nitric oxide; PV: parvalbumin; NMDA: N-methyl-D-aspartate; NFTs: neurofibrillary tangles

Declarations

Authors' contributions

Mincheol Park: Investigation, Methodology, Data curation, Writing-original draft. **Gia Minh Hoang:** Investigation, Methodology, Data curation, Formal analysis, Writing-original draft. **Thien Nguyen**: Conceptualization, Preliminary investigation. **Eunkyung Lee**: Methodology, Sample analysis. **Jae Gwan Kim:** Conceptualization, Supervision, Writing-review & editing. **Tae Kim:** Conceptualization, Supervision, Fund acquisition, Writing-review & editing.

Funding

This work was supported by National Research Foundation of Korea (NRF) grant funded by the Korea government (Ministry of Science and ICT, 2016M3C7A1905475 and 2018R1A2B6006797 to J.G.K, 2017R1A5A1014708 and 2018 R1A2B6002804 to T.K.; Ministry of Education, 2015R1D1A1A01059119 to T.K.); 2021 Joint Research Project of Institutes of Science and Technology to T.K; KBRI basic research program through Korea Brain Research Institute funded by the Ministry of Science and ICT (21-BR-03-05) to J.G.K.

Availability of data and material

The datasets used and/or analysed in the current study are available from the corresponding authors on reasonable request.

Acknowledgements

Not applicable

Ethics approval and consent to participate

All work involving animals approved by the ethics committee at Gwangju Institute of Science and Technology (GIST-2020-031) which is fulfilled with Association for Assessment and Accreditation of Laboratory Animal Care International guidelines.

Consent for publication

All the authors have approved the manuscript.

Competing interests

The authors declare that they have no competing interests

References

1. Alzheimer's Association. 2013 Alzheimer's disease facts and figures. Alzheimer's Dement. 2013;9:208–45.

2. Chiba T, Yamada M, Sasabe J, Terashita K, Shimoda M, Matsuoka M, et al. Amyloid-β causes memory impairment by disturbing the JAK2/STAT3 axis in hippocampal neurons. Mol Psychiatry. 2009;14:206–22.

3. Hardy J, Selkoe DJ. The Amyloid Hypothesis of Alzheimer's Disease: Progress and Problems on the Road to Therapeutics. Science. 2002;297:353-6.

4. Masters CL, Bateman R, Blennow K, Rowe CC, Sperling RA, Cummings JL. Alzheimer's disease. Nat Rev Dis Prim. 2015;1:15056.

5. Zlokovic B V. Neurovascular pathways to neurodegeneration in Alzheimer's disease and other disorders. Nat Rev Neurosci. 2011;12:723–38.

6. Weller RO, Subash M, Preston SD, Mazanti I, Carare RO. SYMPOSIUM: Clearance of Aβ from the Brain in Alzheimer's Disease: Perivascular Drainage of Amyloid-β Peptides from the Brain and Its Failure in Cerebral Amyloid Angiopathy and Alzheimer's Disease. Brain Pathol. 2008;18:253–66.

7. Cserr HF, Harling-Berg CJ, Knopf PM. Drainage of brain extracellular fluid into blood and deep cervical lymph and its immunological significance. Brain Pathol. 1992;2:269–76.

8. Cummings J, Lee G, Ritter A, Sabbagh M, Zhong K. Alzheimer's disease drug development pipeline. Alzheimer's Dement Transl Res Clin Interv. 2020;6:e12050.

9. Mehta D, Jackson R, Paul G, Shi J, Sabbagh M. Why do trials for Alzheimer's disease drugs keep failing? A discontinued drug perspective for 2010-2015. Expert Opin Investig Drugs. 2017;26:735–9.

10. Abbott A, Dolgin E. Leading Alzheimer's theory survives drug failure. Nature. 2016;540:15–6.

11. Kaiser J, Lutzenberger W. Induced Gamma-Band Activity and Human Brain Function. Neuroscientist. 2003;9:475–84.

12. Colgin LL, Moser EI. Gamma Oscillations in the Hippocampus. Physiology. 2010;25:319–29.

13. Traub RD, Whittington MA, Stanford IM, Jefferys JGR. A mechanism for generation of long-range synchronous fast oscillations in the cortex. Nature. 1996;383:621–4.

14. Carlén M, Meletis K, Siegle JH, Cardin JA, Futai K, Vierling-Claassen D, et al. A critical role for NMDA receptors in parvalbumin interneurons for gamma rhythm induction and behavior. Mol Psychiatry. 2012;17:537–48.

15. Sohal VS, Zhang F, Yizhar O, Deisseroth K. Parvalbumin neurons and gamma rhythms enhance cortical circuit performance. Nature. 2009;459:698–702.

16. Palop JJ, Chin J, Roberson ED, Wang J, Thwin MT, Bien-Ly N, et al. Aberrant Excitatory Neuronal Activity and Compensatory Remodeling of Inhibitory Hippocampal Circuits in Mouse Models of Alzheimer's Disease. Neuron. 2007;55:697–711.

17. Verret L, Mann EO, Hang GB, Barth AMI, Cobos I, Ho K, et al. Inhibitory Interneuron Deficit Links Altered Network Activity and Cognitive Dysfunction in Alzheimer Model. Cell. 2012;149:708–21.

18. Gillespie AK, Jones EA, Lin Y-H, Karlsson MP, Kay K, Yoon SY, et al. Apolipoprotein E4 Causes Age-Dependent Disruption of Slow Gamma Oscillations during Hippocampal Sharp-Wave Ripples. Neuron. 2016;90:740–51.

19. Mably AJ, Colgin LL. Gamma oscillations in cognitive disorders. Curr Opin Neurobiol. 2018;52:182–7.

20. Stam CJ, van Cappellen van Walsum AM, Pijnenburg YAL, Berendse HW, de Munck JC, Scheltens P, et al. Generalized Synchronization of MEG Recordings in Alzheimer's Disease: Evidence for Involvement of the Gamma Band. J Clin Neurophysiol. 2002;19.

21. Koenig T, Prichep L, Dierks T, Hubl D, Wahlund LO, John ER, et al. Decreased EEG synchronization in Alzheimer's disease and mild cognitive impairment. Neurobiol Aging. 2005;26:165–71.

22. Stam CJ, Van Der Made Y, Pijnenburg YAL, Scheltens P. EEG synchronization in mild cognitive impairment and Alzheimer's disease. Acta Neurol Scand. 2003;108:90–6.

23. Iaccarino HF, Singer AC, Martorell AJ, Rudenko A, Gao F, Gillingham TZ, et al. Gamma frequency entrainment attenuates amyloid load and modifies microglia. Nature. 2016;540:230–5.

24. Martorell AJ, Paulson AL, Suk H-J, Abdurrob F, Drummond GT, Guan W, et al. Multi-sensory Gamma Stimulation Ameliorates Alzheimer's-Associated Pathology and Improves Cognition. Cell. 2019;177:256-71.

25. Eguchi K, Shindo T, Ito K, Ogata T, Kurosawa R, Kagaya Y, et al. Whole-brain low-intensity pulsed ultrasound therapy markedly improves cognitive dysfunctions in mouse models of dementia - Crucial roles of endothelial nitric oxide synthase. Brain Stimul. 2018;11:959–73.

26. Huang X, Lin Z, Wang K, Liu X, Zhou W, Meng L, et al. Transcranial Low-Intensity Pulsed Ultrasound Modulates Structural and Functional Synaptic Plasticity in Rat Hippocampus. IEEE Trans Ultrason Ferroelectr Freq Control. 2019;66:930–8.

27. Lee Y, Choi Y, Park E-J, Kwon S, Kim H, Lee JY, et al. Improvement of glymphatic–lymphatic drainage of beta-amyloid by focused ultrasound in Alzheimer's disease model. Sci Rep. 2020;10:16144.

28. Bobola MS, Chen L, Ezeokeke CK, Olmstead TA, Nguyen C, Sahota A, et al. Transcranial focused ultrasound, pulsed at 40 Hz, activates microglia acutely and reduces Aβ load chronically, as demonstrated in vivo. Brain Stimul. 2020;13:1014–23.

29. Jones RSG, Bühl EH. Basket-like interneurones in layer II of the entorhinal cortex exhibit a powerful NMDA-mediated synaptic excitation. Neurosci Lett. 1993;149:35–9.

30. Brown MR, Radford SE, Hewitt EW. Modulation of β-Amyloid Fibril Formation in Alzheimer's Disease by Microglia and Infection. Front Mol Neurosci. 2020;13:609073.

31. Bamberger ME, Harris ME, McDonald DR, Husemann J, Landreth GE. A Cell Surface Receptor Complex for Fibrillar β-Amyloid Mediates Microglial Activation. J Neurosci. 2003;23:2665-74.

32. Heneka MT, Golenbock DT, Latz E. Innate immunity in Alzheimer's disease. Nat Immunol. 2015;16:229–36.

33. Yankner BA, Lu T. Amyloid β-Protein Toxicity and the Pathogenesis of Alzheimer Disease*,. J Biol Chem. 2009;284:4755–9.

34. Meyer-Luehmann M, Spires-Jones TL, Prada C, Garcia-Alloza M, de Calignon A, Rozkalne A, et al. Rapid appearance and local toxicity of amyloid-β plaques in a mouse model of Alzheimer's disease. Nature. 2008;451:720–4.

35. Chen G, Xu T, Yan Y, Zhou Y, Jiang Y, Melcher K, et al. Amyloid beta: structure, biology and structure-based therapeutic development. Acta Pharmacol Sin. 2017;38:1205–35.

36. Jin M, Shepardson N, Yang T, Chen G, Walsh D, Selkoe DJ. Soluble amyloid β-protein dimers isolated from Alzheimer cortex directly induce Tau hyperphosphorylation and neuritic degeneration. Proc Natl Acad Sci. 2011;108:5819–24.

37. Gharibyan AL, Zamotin V, Yanamandra K, Moskaleva OS, Margulis BA, Kostanyan IA, et al. Lysozyme Amyloid Oligomers and Fibrils Induce Cellular Death via Different Apoptotic/Necrotic Pathways. J Mol Biol. 2007;365:1337–49.

38. Rajji TK, Zomorrodi R, Barr MS, Blumberger DM, Mulsant BH, Daskalakis ZJ. Ordering information in working memory and modulation of mamma by theta oscillations in humans. Cereb Cortex. 2017;27:1482–90.

39. Lisman JE, Jensen O. The Theta-Gamma Neural Code. Neuron. 2013;77:1002–16.

40. Goodman MS, Kumar S, Zomorrodi R, Ghazala Z, Cheam ASM, Barr MS, et al. Theta-Gamma Coupling and Working Memory in Alzheimer's Dementia and Mild Cognitive Impairment. Front. Aging Neurosci. . 2018. p. 101.

41. Grigorovsky V, Jacobs D, Breton VL, Tufa U, Lucasius C, del Campo JM, et al. Delta-gamma phase-amplitude coupling as a biomarker of postictal generalized EEG suppression. Brain Commun. 2020;2:fcaa182.

Figures

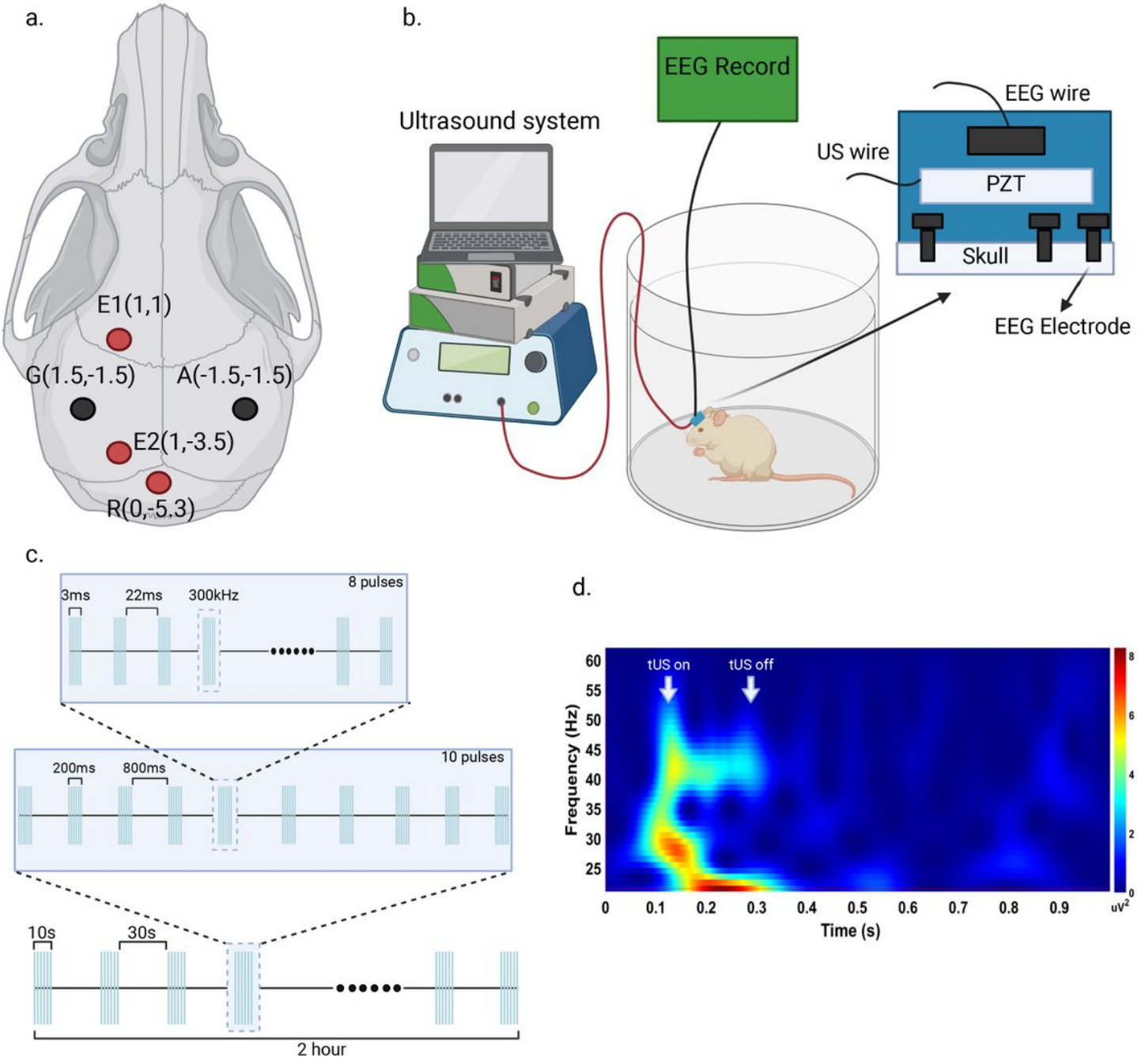

Figure 1

Experiment protocol. (a) EEG electrode positions for surgical implantation. (b) tUS and EEG record device setup. (c) Ultrasound parameter protocol. (d) Time-frequency distribution of brain activity generated by tUS.

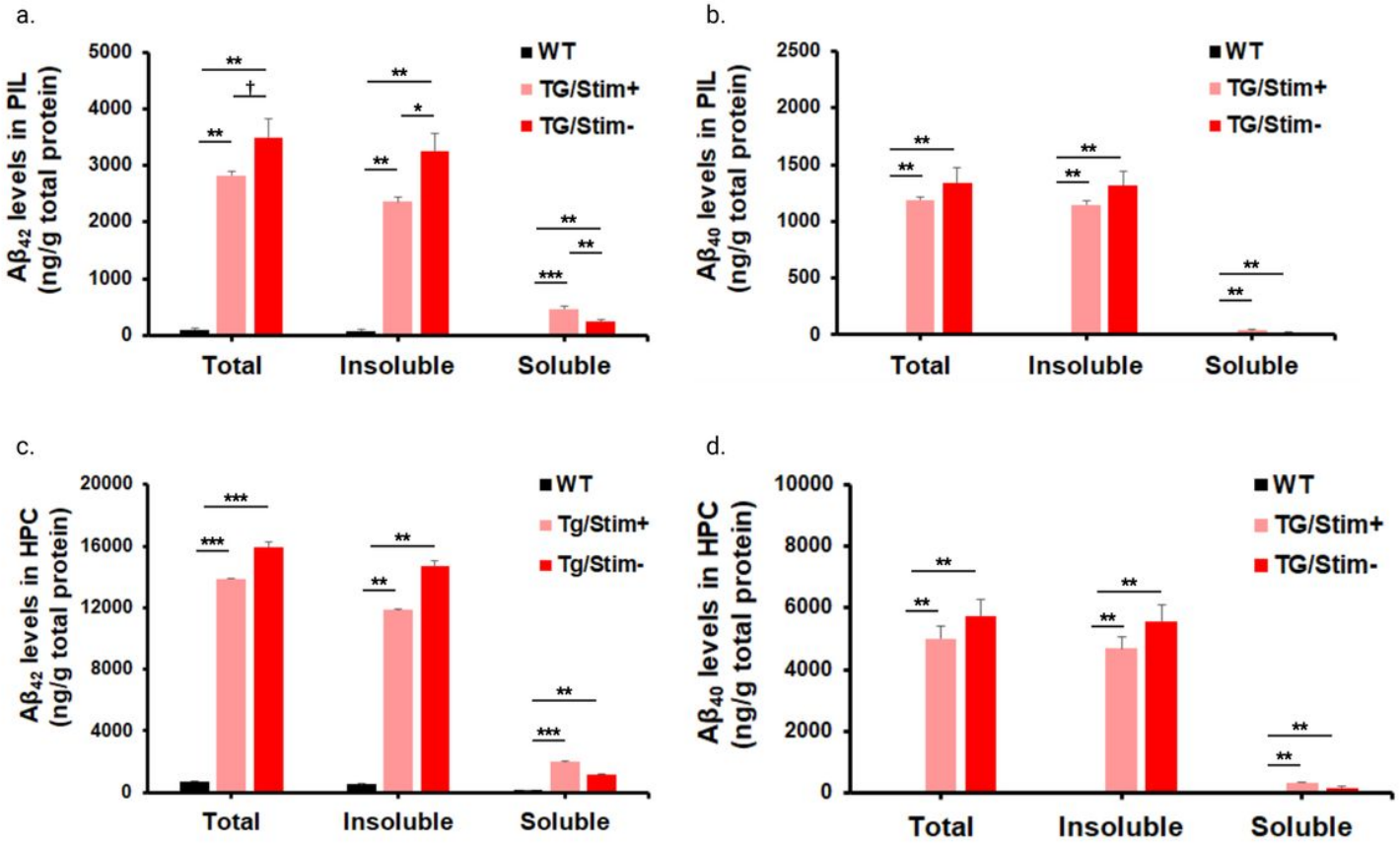

Figure 2

Aβ load in the pre- and infra-limbic cortex and the hippocampus changed after two weeks of ultrasound stimulation. (a) Aβ42 levels in the pre- and infra-limbic cortex. (b) Aβ40 levels in the pre- and infra-limbic cortex. (c) Aβ42 levels in the hippocampus. (d) Aβ40 levels in the hippocampus. Black, pink, and red bars indicate mice groups of wild type (WT), 5xFAD with stimulation (Tg/Stim+), and 5XFAD sham stimulation (Tg/Stim-), respectively. PIL, pre- and infra-limbic cortex; HPC, hippocampus; *p<0.05, **p< 0.01, ***p<0.001 following paired sample t-test for normally distributed data, † p<0.05 following Mann-Whitney Rank Sum Test for non-normally distributed data.

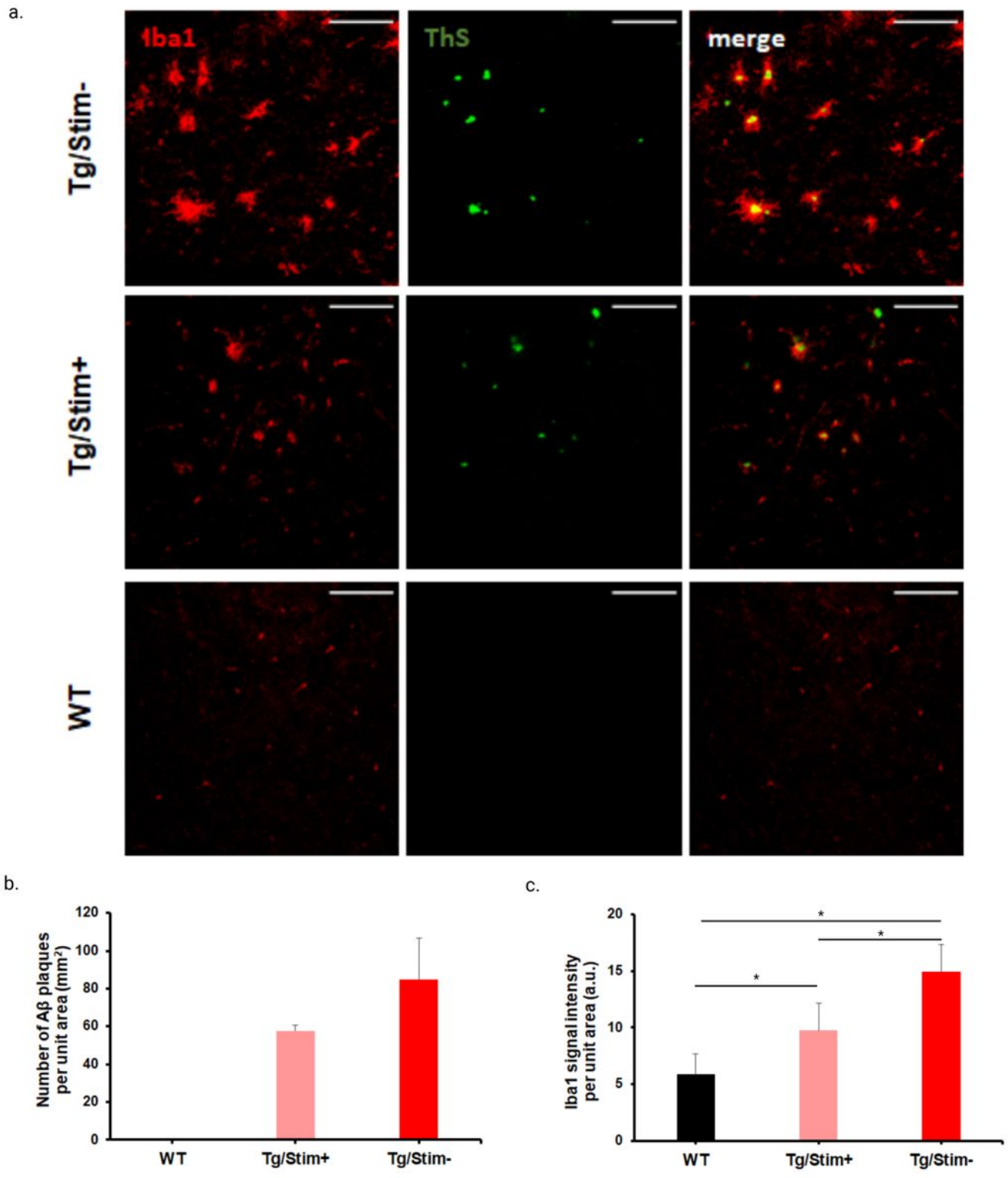

Figure 3

The signal intensity of microglia changed after two weeks of ultrasound stimulation. (a) Representative images of microglia and Aβ plaque in PIL. (Scale bar = 100 μm). (b) The number of Aβ plaque per unit area (mm2) in PIL cortex. (c) Iba1 signal intensity per unit area (a.u.) in PIL cortex. Black, pink, and red bars indicate mice groups of wild type (WT), 5xFAD with stimulation (Tg/Stim+), and 5XFAD sham stimulation (Tg/Stim-), respectively. PIL, pre- and infra-limbic cortex; *p<0.05, **p< 0.01, ***p<0.001

following paired sample t-test for normally distributed data, † p<0.05 following Mann-Whitney Rank Sum Test for non-normally distributed data.

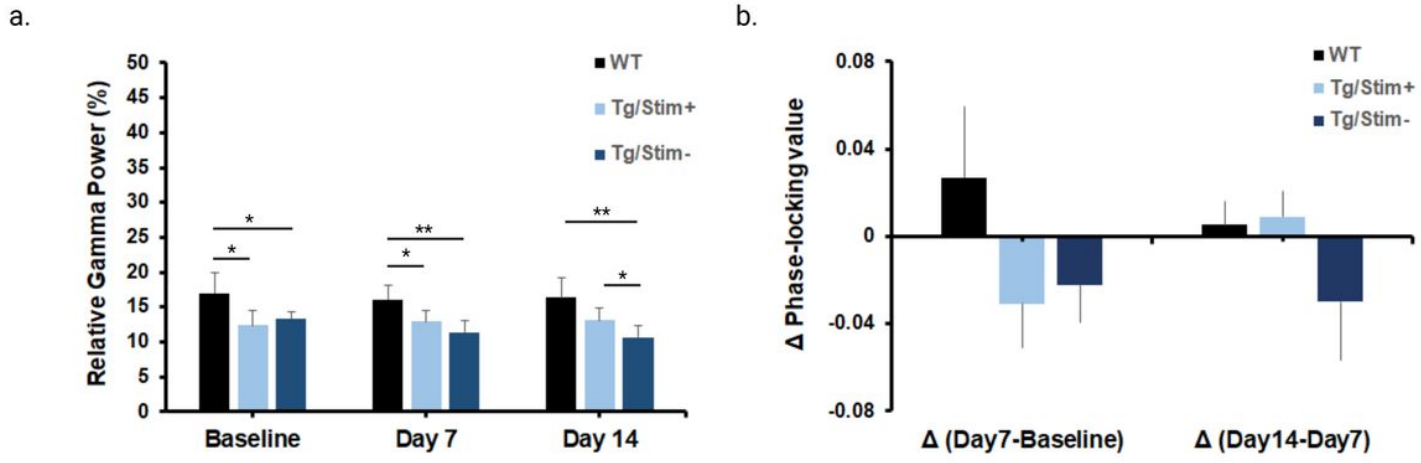

Figure 4

Spontaneous gamma power and phase-locking value increased after two weeks of ultrasound stimulation. (a) EEG gamma power relative to total power. (b) Change of phase-locking value from baseline to stimulation day 14. WT, wild type; Tg/Stim+, 5XFAD with stimulation; Tg/Stim-, 5XFAD with sham stimulation; *p<0.05, **p< 0.01 following two-sample (independent) t-test.

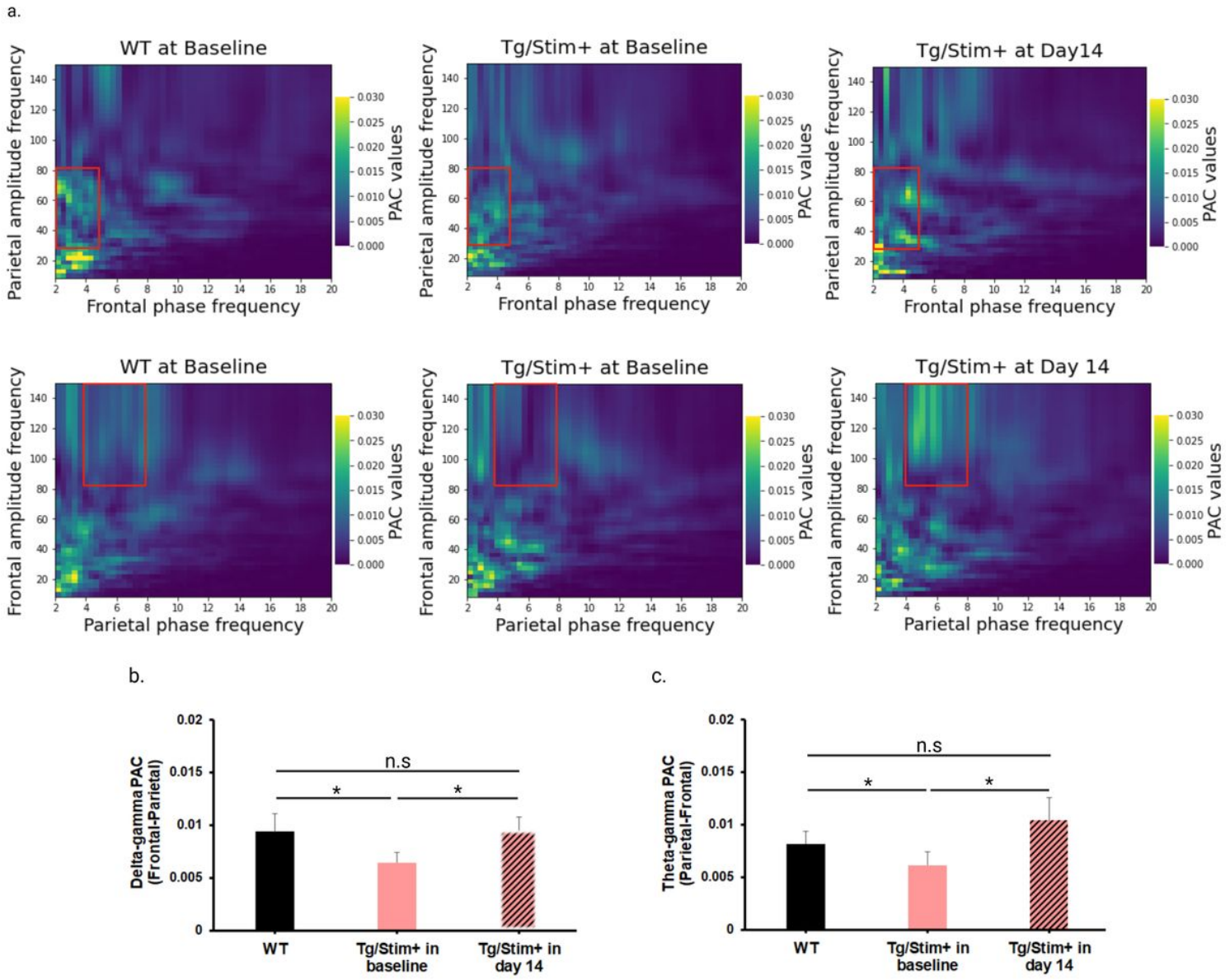

Figure 5

Cross-frequency phase-amplitude coupling improved after 2 weeks of ultrasound stimulation. (a) Cross-frequency phase-amplitude coupling (PAC) of the frontal and parietal. Parietal amplitude frequency and frontal phase frequency coupling (upper row) and frontal amplitude frequency and parietal phase frequency coupling (bottom row) was plotted. Red rectangles represent the area of interest (ROI). (b-c) Delta-gamma and theta-gamma PAC. WT, wild type; Tg/Stim+, 5XFAD with stimulation; Tg/Stim-, 5XFAD with sham stimulation; n.s., no significance; *p<0.05, **p< 0.01 following two-sample (independent) t-test.